ACS OMEGA

Open Access

http://pubs.acs.org/journal/acsodf

Article

Synthesis, Biological Properties, and Molecular Docking Study of Novel 1,2,3-Triazole-8-quinolinol Hybrids

Mohamed El Faydy, Loubna Lakhrissi, Naoufel Dahaieh, Khadija Ounine, Burak Tüzün, Nabila Chahboun, Ahmed Boshaala, Abeer AlObaid, Ismail Warad, Brahim Lakhrissi, and Abdelkader Zarrouk*

Cite This: *ACS Omega* 2024, 9, 25395−25409

Read Online

ACCESS | Metrics & More | Article Recommendations | Supporting Information

ABSTRACT: A new series of 1,2,3-triazole-8-quinolinol hybrids were synthesized in good yields using monosubstituted acetonitriles and 5-azidomethyl-8-quinolinol as the starting reagents via a one-step protocol. The structures of 1,2,3-triazole-8-quinolinol hybrids were characterized by nuclear magnetic resonance (^{1}H and ^{13}C NMR) spectroscopy and elemental analysis. Antibacterial activity in vitro of all the synthesized hybrids was investigated against *Escherichia coli* (*E. coli*), *Xanthomonas fragariae* (*X. fragariae*), *Staphylococcus aureus* (*S. aureus*), and *Bacillus subtilis* (*B. subtilis*) applying the methods of disk diffusion and minimal inhibition concentration (MIC). Hybrid **7** exhibited excellent antibacterial capacity, with an MIC value of 10 μg/mL against *S. aureus* and 20 μg/mL against *B. subtilis*, *E. coli*, and *X. fragariae*, which were comparable to those that of the standard antibiotic nitroxoline. A structure−activity relationship (SAR) study of 1,2,3-triazole-8-quinolinol hybrids showed that introducing electron-donating substituents in the 1,2,3-triazole ring at the 4-position is important for activity. Quantum chemical calculations have been undertaken to employ the Gaussian software in the B3LYP, HF, and M062X basis sets using 3-21g, 6-31g, and SDD levels to further explain linkages within the antibacterial findings. Furthermore, molecular docking investigations were also conducted to investigate the binding affinities as well as the interactions of some hybrids with the target proteins. An absorption, distribution, metabolism, excretion, and toxicity (ADME/T) investigation was carried out to scrutinize the viability of employing the 1,2,3-triazole-8-quinolinol hybrids as medicines.

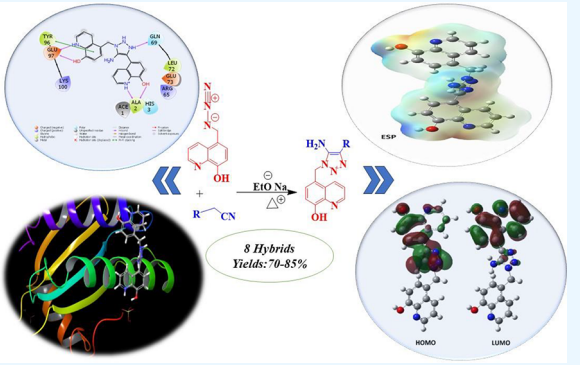

1. INTRODUCTION

Antimicrobial resistance poses a significant threat to human health in the field of contagious diseases inflicted by viruses, parasites, bacteria, and fungi. Antibiotic-resistant infections produce dangerous diseases, hospitalize patients for extended periods of time, increase medical costs, and cause treatment failures. It is estimated that approximately 700,000 deaths worldwide are attributed to antimicrobial resistance each year, and this may increase to 10 million cases per year by 2050.[1] It is for this reason that the discovery of novel, effective antimicrobial agents is necessary to dominate the proliferation of these pathogens.

1,2,3-Triazole, which can act as the isostere of amide, ester, carboxylic acid, and other heterocycles, is a common pharmacophore in many drugs[2] and has a wide range of pharmacological properties, including antitubercular,[3−9] antifungal,[10,11] antitumor,[12,13] and antibacterial[14,15] activities. These properties are attributed to the 1,2,3-triazole moiety, which can exert various noncovalent interactions that can enhance the solubility and ability to bind to bimolecular targets.[16] As a result, 1,2,3-triazole derivatives play an intriguing role in developing new drugs.

Hybrid molecules are chemical entities that have two or more structural domains with different biological roles and dual activities, signifying that a hybrid molecule operates as two or more distinct pharmacophores.[17,18] Hybrid molecules have the potential to minimize toxicity, widen the biological range, overcome drug cross-resistance, and improve efficacy compared to the parent drugs.[19,20] In the last three decades, numerous hybrid molecules, such as Ro 23−9424 and TD-1792, have been clinically tested for the treatment of different diseases,[21,22] demonstrating the relevance of hybrid molecules in the development of new drugs. Hybridization of 1,2,3-triazole with other antibacterial pharmacophores may provide new

Received: April 23, 2024
Revised: May 22, 2024
Accepted: May 24, 2024
Published: May 31, 2024

candidates with excellent potency against both drug-sensitive and drug-resistant bacteria.

Quinolines, especially 8-quinolinol, are common pharmacophores in antibacterial agents.[23−26] They attracted the attention of medicinal and organic chemists to synthesize target-based drugs by inserting various substituents in positions 5, 7, or 8 so that the drug molecule binds to the target site selectively or more effectively with little or no toxicity to normal cells.[27,28] Also, the insertion of electron-donating groups and/or halogen atoms into these heterocyclic molecules can enhance the growth-inhibitory influence.[29] Nonetheless, some reports indicate that the hybridization of 8-quinolinol with other antibacterial pharmacophores has resulted in increased antibacterial efficacy.[30,31]

Theoretical computations constitute one of the most often-used methodologies nowadays. However, theoretical computations have become more feasible and speedier as technology has advanced.[32−35] Gaussian software and the Maestro Molecular Modeling Platform by Schrödinger are the two most used programs in theoretical calculations. Initially, the chemical characteristics of the molecules were probed through calculations employing the B3LYP, HF, and M06−2x approaches via the 3-21g, 6-31g, and SDD basis sets.[36−38] Following that, their biological features against diverse bacteria's proteins were under scrutiny, including the crystal structure of *Staphylococcus aureus* (PDB ID: 1JIJ),[39] the crystal structure of *Bacillus subtilis* (PDB ID: 1A6F),[40] and the crystal structure of *Escherichia coli* K-12 (PDB ID: 4WUB).[41] In addition to these, the prospect of being utilized as a medicine was examined by analyzing the drug characteristics of 1,2,3-triazole-8-quinolinol hybrids. For this, ADME/T analysis was undertaken.

Obviously, hybridizing 1,2,3-triazole with 8-quinolinol is a promising strategy for developing novel antibacterial candidates, and to our knowledge, the antibacterial effects of 1,2,3-triazole hybridized with 8-quinolinol derivatives on bacterial growth inhibition have rarely been investigated. Accordingly, the aim of this work was to synthesize and characterize new 1,2,3-triazole-8-quinolinol hybrids, evaluate their antibacterial activities against various pathogenic microorganisms, including both Gram-positive and Gram-negative bacteria, using the agar diffusion method (disk diffusion method), and determine their minimum inhibitory concentrations (MIC). The novelty of the present study lies in synthesizing 1,2,3-triazole-8-quinolinol hybrids in a one-pot process in good yield from easily available precursors under mild conditions. Theoretical computations, together with molecular docking analyses, are used to correlate the structural characteristics of the studied hybrids with their antibacterial activities.

2. EXPERIMENTAL SECTION

2.1. Reagents and Apparatus. All lab products were received from Sigma-Aldrich. ^{1}H and ^{13}C NMR spectra were logged via a Bruker spectrometer (300 MHz) with dimethyl sulfoxide-d_6 ($(CD_3)_2S{=}O$) as solvent. The reaction progression was identified on the Merck TLC Plate Silica Gel 60 F254. Silica gel (particle size 0.040−0.063 mm) was used for column chromatography. Analysis of C, H, and N elements was performed utilizing PerkinElmer EA 2400 II. Melting points were determined by Banc Kofler Wagner & Muntz.

2.2. General Procedure for the Synthesis of 1,2,3-Triazole-8-quinolinol Hybrids. A mixture of 5-azidomethyl-8-quinolinol (1 g, 1.4 mmol), monosubstituted acetonitriles (1.3 g, 1.8 mmol), and sodium ethanolate (1 g, 1.4 mmol) was solubilized in 30 mL of abs. ethanol and refluxed for 24 h. Then, the ethanol was evaporated, and the residue obtained was hydrolyzed with 20 mL of water saturated with NaCl and extracted with chloroform (3 × 20 mL). The organic fractions were dehydrated with Na_2SO_4 and evaporated. The raw product was purified through silica gel column chromatography with petroleum ether (60−80 °C) and acetone (9:1−3:7, v/v) to provide a white powder in high yield for all prepared hybrids.

*2.2.1. 4-Amino-1-((8-quinolinol-5-yl)methyl)-1,2,3-triazole-5-carbonitrile (**2**).*

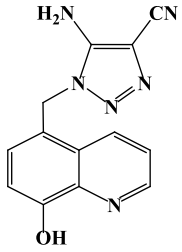

As a black powder; Yield 76%; m.p.: 125 ± 2 °C.

^{1}H NMR (300 MHz, $(CD_3)_2S{=}O$, δppm): 8.99 (d, 1H, Ar−H), 8.82 (d, 1H, Ar−H), 7.54 (t, 1 H, Ar−H), 7.24 (d, 1 H, Ar−H), 6.97 (d, 1 H, Ar−H), 6.16 (s, 2H, C−H), 7.87 (s, 2H, N−H).

^{13}C NMR (300 MHz, $(CD_3)_2S{=}O$, δppm): 111.32 (CN), 37.18 (CH_2), 122.29, 127.84, 128.95, 133.78, 148.37 (Ar−CH), 127.92, 129.30, 136.37, 138.04, 139.67, 152.74 (Ar−C).

Elemental analysis Calcd for (C13H10N6O, %): C,58.64; H, 3.79; N, 31.56%. Found for ($C_{16}H_{11}N_3O$, %): C, 58.56; H, 3.70; N, 31.70.

*2.2.2. Methyl 4-amino-1-((8-quinolinol-5-yl)methyl)-1,2,3-triazole-5-carboxylate (**4**).*

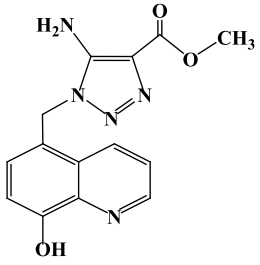

As a white powder; yield 73%; m.p.: 155 ± 2 °C.

^{1}H NMR (300 MHz, $(CD_3)_2S$ = O, δppm): 8.85 (d, 1H, Ar−H), 8.51 (d, 1H, Ar−H), 7.60 (t, 1H, Ar−H), 7.52 (d, 1H, Ar−H), 7.04 (d, 1H, Ar−H), 5.48 (s, 2H, C−H), 8.08 (s, 2H, N−H), 3.95 (s, 3H, C−H).

^{13}C NMR (300 MHz, $(CD_3)_2S{=}O$, δppm): 169.17 (C═O), 66.02 (CH_3), 61.16 (CH_2), 109.90, 122.02, 131.35, 136.48, 149.16 (Ar−CH), 153.26, 139.33, 138.95, 133.08, 127.63, 125.74 (Ar−C).

Elemental analysis calcd for ($C_{14}H_{13}N_5O_3$, %): C,56.18; H, 4.38; N, 23.40%. Found for ($C_{14}H_{13}N_5O_3$, %): C, 55.84; H, 3.90; N, 24.05.

https://doi.org/10.1021/acsomega.4c03906
ACS Omega 2024, 9, 25395−25409

*2.2.3. Ethyl-4-amino-1-((8-quinolinol-5-yl)methyl)-1H-1,2,3-triazole-5-carboxylate (**3**).*

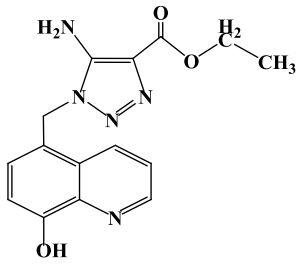

As a white powder; yield 71%; m.p.: 162 ± 2 °C.

^{1}H NMR (300 MHz, $(CD_3)_2S$ = O, δppm): 8.86 (d, 1H, Ar−H), 8.49 (d, 1H, Ar−H), 7.56 (t, 1H, Ar−H), 7.46 (d, 1H, Ar−H), 7.06 (d, 1H, Ar−H), 7.99 (s, 2H, N−H), 5.73 (s, 2H, C−H), 1.19 (t, 3H, C−H), 4.158 (q, 2H, C−H)

^{13}C NMR (300 MHz, $(CD_3)_2S$ = O, δppm): 168.69 (C = O), 13.852 (CH_3), 62.839 (CH_2), 53.86 (CH_2), 111.02, 119.44, 121.75, 133.94, 148.37 (Ar−CH), 153.53, 139.59, 137.99, 129.91, 128.29, 121.86 (Ar−C).

Elemental analysis Calcd for ($C_{15}H_{15}N_5O_3$, %): C, 57.50; H, 4.83; N, 22.35%. Found for ($C_{15}H_{15}N_5O_3$, %): C, 58.03; H, 4.33; N, 21.96.

*2.2.4. 5-amino-1-((8-quinolinol-5-yl)methyl)-1H-1,2,3-triazole-4-carboxamide (**6**).*

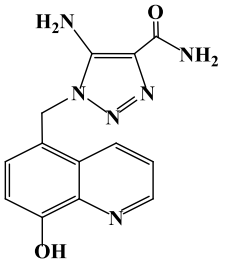

As a white powder; Yield 75%; m.p.: 145 ± 2 °C.

^{1}H NMR (300 MHz, $(CD_3)_2S$=O, δppm): 8.85 (d, 1H, Ar−H), 8.46 (d, 1H, Ar−H), 7.59 (t, 1H, Ar−H), 7.45 (d, 1H, Ar−H), 7.03 (d, 1H, Ar−H), 6.64 (s, 2H, N−H), 7.97 (s, 2H, N−H), 5.31 (s, 2H, C−H).

^{13}C NMR (300 MHz, $(CD_3)_2S$=O, δppm): 166.983 (C=O), 53.705 (CH_2), 111.05, 117.55, 122.28, 133.00, 148.39 (Ar−CH), 153.39, 139.10, 135.77, 129.43, 127.56, 122.58 (Ar−C).

Elemental analysis calcd for ($C_{13}H_{12}N_6O_2$, %): C,54.93; H, 4.25; N, 29.56%. Found for ($C_{13}H_{12}N_6O_2$, %): C, 55.15; H, 4.19; N, 30.09.

*2.2.5. 1-(5-Amino-1-((8-quinolinol-5-yl)methyl)-1H-1,2,3-triazol-4-yl)ethanone (**5**).*

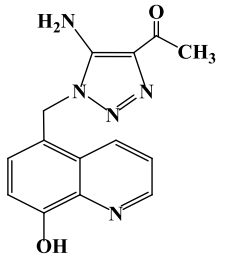

As a white powder; yield 75%; m.p.: 158 ± 2 °C.

^{1}H NMR (300 MHz, $(CD_3)_2S$=O, δppm): 8.84 (d, 1H, Ar−H), 8.44 (d, 1H, Ar−H), 7.56 (t, 1H, Ar−H), 7.45 (d, 1H, Ar−H), 7.03 (d, 1H, Ar−H), 8.11 (s, 2H, N−H), 1.08 (s, 3H, C−H), 4.72 (s, 2H, C−H).

^{13}C NMR (300 MHz, $(CD_3)_2S$=O, δppm): 168.93 (C=O), 46.18 (CH_2), 111.32, 122.29, 127.92, 133.78, 148.37 (Ar−CH), 127.84, 129.30, 136.37, 138.04, 139.68, 152.74 (Ar−C), 24.65 (CH_3).

Elemental analysis calcd for ($C_{14}H_{13}N_5O_2$, %): C,59.36; H, 4.63; N, 24.72%. Found: C, 60.01; H, 4.39; N, 25.11.

*2.2.6. 5-((5-Amino-4-phenyl-1H-1,2,3-triazol-1-yl)methyl)-8-quinolinol (**8**).*

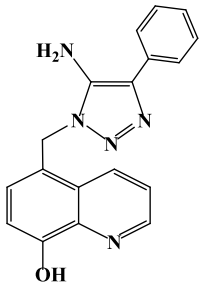

As a white powder; yield 86%; m.p.: 160 ± 2 °C.

^{1}H NMR (300 MHz, $(CD_3)_2S$=O, δppm): 8.81 (d, 1H, Ar−H), 8.59 (d, 1H, Ar−H), 7.54 (t, 1H, Ar−H), 7.32 (d, 1H, Ar−H), 6.78 (d, 1H, Ar−H), 7.33 (s, 2H, N−H), 5.94 (s, 2H, C−H), 6.67 (t, 1H, Ar−H), 7.25 (t, 2H, Ar−H), 6.97 (d, 2H, Ar−H)

^{13}C NMR (300 MHz, $(CD_3)_2S$=O, δppm): 54.50 (CH_2), 110.35, 121.96, 129.13, 129.70, 131.87, 132.00, 132.53, 148.37 (Ar−CH), 153.66, 139.10, 134.68, 132.49, 129.29, 128.49, 124.24 (Ar−C).

Elemental analysis Calcd for ($C_{18}H_{15}N_5O$, %): C,68.13; H, 4.76; N, 22.07%. Found: C, 67.81; H, 4.39; N, 23.11.

*2.2.7. 5-(5-Amino-1-((8-quinolinol-5-yl)methyl)-1H-1,2,3-triazol-4-yl)-8-quinolinol (**7**).*

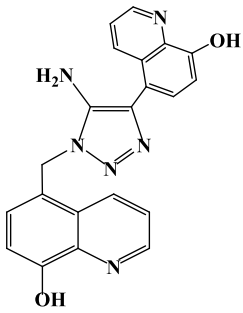

As a white powder; yield 78%; m.p.: 147 ± 2 °C.

^{1}H NMR (300 MHz, $(CD_3)_2S$=O, δppm): 8.80 (d, 1H, Ar−H), 8.39 (d, 1H, Ar−H), 7.49 (t, 1H, Ar−H), 7.20 (d, 1H, Ar−H), 6.95 (d, 1H, Ar−H), 8.79 (d, 1H, Ar−H), 8.22 (d, 1H, Ar−H), 7.29 (t, 1H, Ar−H), 7.03 (d, 1H, Ar−H), 6.93 (d, 1H, Ar−H), 6.92 (s, 2H, N−H), 4.23 (s, 2H, C−H).

^{13}C NMR (300 MHz, $(CD_3)_2S$=O, δppm): 43.63 (CH_2), 110.74, 110.95, 116.01, 116.09, 122.31, 122.43, 127.50, 127.83, 148.29, 148.51 (Ar−CH), 153.51, 153.39, 139.27, 139.23, 132.80, 132.97, 127.45, 127.01, 124.87, 123.52 (Ar−C).

Elemental analysis calcd for ($C_{21}H_{16}N_6O_2$, %): C,65.62; H, 4.20; N, 21.86%. Found: C, 64.89; H, 4.19; N, 22.31.

https://doi.org/10.1021/acsomega.4c03906
ACS Omega 2024, 9, 25395−25409

Scheme 1. Synthesis of 1,2,3-Triazole-8-quinolinol Hybrids (2−9)

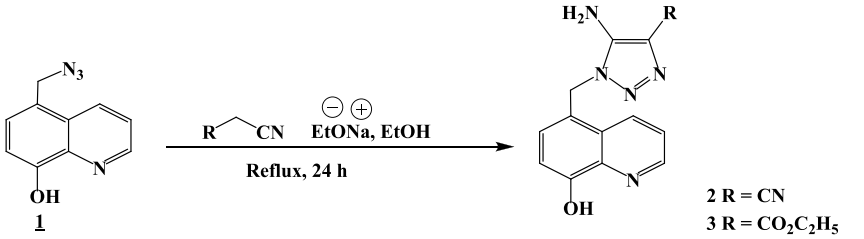

*2.2.8. 5-((5-Amino-4-chloro-1H-1,2,3-triazol-1-yl)methyl)-8-quinolinol (**9**).*

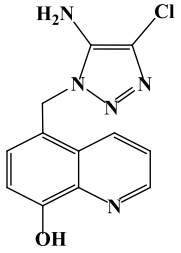

As a white powder; yield 85%; m.p.: 129 ± 2 °C.

^{1}H NMR (300 MHz, $(CD_3)_2S{=}O$, δppm): 8.93 (d, 1H, Ar−H), 8.66 (d, 1H, Ar−H), 7.69 (t, 1H, Ar−H), 7.15 (d, 1H, Ar−H), 6.96 (d, 1H, Ar−H), 7.93 (s, 2H, N−H), 5.76 (s, 2H, C−H).

^{13}C NMR (300 MHz, $(CD_3)_2S{=}O$, δppm): 49.39 (CH_2), 110.62, 118.20, 122.34, 127.93, 133.47, 148.37 (Ar−CH), 154.02, 142.15, 139.12, 129.47, 124.36 (Ar−C).

Elemental analysis calcd for ($C_{12}H_{10}N_5OCl$, %): C, 52.28; H, 3.66; N, 25.40%. Found: C, 51.79; H, 4.10; N, 25.85.

2.3. Pharmacological Screening. The antibacterial effect of prepared 1,2,3-triazole-8-quinolinol hybrids was examined in vitro for restraining the growth of some pathogens by applying the diffusion method employing Mueller Hinton agar. The antibacterial potential was screened against two Gram-negative microorganisms, including *Escherichia coli* and *Xanthomonas fragariae*, and two Gram-positive microorganisms, *Staphylococcus aureus* and *Bacillus subtilis*. The employed microorganisms were provided by the Laboratory of Nutrition, Health, and Environment, Faculty of Sciences, Ibn Tofaïl University, Kenitra (Morocco). 6 mm-diameter sterilized filter paper disks were dipped in the solution to be tested (at a concentration of 100 μg/mL in dimethyl sulfoxide (DMSO) (1%)) and then placed in the midst of each inoculated plate. After that, the plates were incubated for 24 h at 37 °C. The read of the data was realized by measuring the inhibition zone diameter produced by the test substance utilizing a ruler. Nitroxoline was employed as a reference drug.

The agar dilution approach was employed to figure out the minimum inhibitory concentration (MIC). Solutions of the synthesis hybrids to be tested (100 μg/mL in DMSO), 96 deep well plates, Muller−Hinton broth, and suspensions of microorganisms (0.5 McFarland) were utilized as materials. The prepared doses of the tested hybrids range between 100 and 10 μg/mL. After incubation at 37 °C for 24 h, the MIC value for every prepared hybrid was established by macroscopic observation of microbial growth. It corresponds to the well with the weakest dose of the prepared hybrid, in which the growth of microorganisms is significantly inhibited.

2.4. Theoretical Methods. Theoretical computations are undertaken to assess the chemical and biological characteristics of substances. When studying the chemical characteristics of molecules, several quantum chemical parameters are determined.[41−44] Each variable provides details concerning various molecular features. These variables were computed through Gaussian 09 RevD.01 and GaussView 6.0.[45,46] The aforementioned programs were adopted to carry out computations for molecules at the B3LYP, HF, and M06−2x levels through the 3-21g, 6-31g, and SDD basis sets.[36−38] Several quantum chemical variables, including HOMO (highest occupied molecular orbital), LUMO (lowest unoccupied molecular orbital), ΔE (HOMO−LUMO energy gap), chemical potential (μ), electrophilicity (ω), chemical hardness (η), global softness (σ), nucleophilicity (ε), and dipole moment, have been computed using eqs 1 to 5, as outlined below:[47−49]

$$\chi = -\left(\frac{\partial E}{\partial N}\right)_{\upsilon(r)} = \frac{1}{2}\left(I + A\right) \cong \frac{1}{2}\left(E_{\mathrm{HOMO}} + E_{\mathrm{LUMO}}\right) \tag{1}$$

$$\eta = -\left(\frac{\partial^2 E}{\partial N^2}\right)_{\upsilon(r)} = \frac{1}{2}\left(I - A\right) \cong \frac{1}{2}\left(E_{\mathrm{HOMO}} - E_{\mathrm{LUMO}}\right) \tag{2}$$

$$\sigma = \frac{1}{\eta} \tag{3}$$

$$\omega = \frac{\chi^2}{2\eta} \tag{4}$$

$$\varepsilon = \frac{1}{\omega} \tag{5}$$

The inhibiting behaviors of the inquired hybrids toward different bacteria proteins were scrutinized in order to study how they function biologically. Schrödinger's Maestro Molecular Modeling Platform (version 12.8) was selected for this analysis.[50] For this computation, the protein preparation module serves for protein structure creation,[51] the LigPrep module[52] serves for the elaboration of molecules, and the Glide ligand docking module is employed for the interaction among the molecules and proteins.[53]

https://doi.org/10.1021/acsomega.4c03906
ACS Omega 2024, 9, 25395−25409

Scheme 2. Proposed Reaction Mechanism for Synthesizing 1,2,3-Triazole-8-quinolinol Hybrids

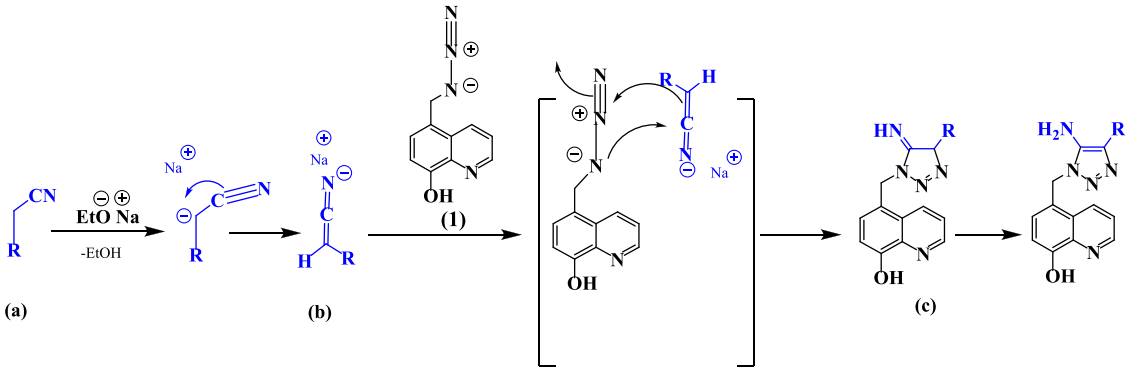

However, the research was done utilizing ADME/T analysis so that the examined hybrids may be employed as medications. The Qik-prop module of the Schrödinger program was employed to forecast the effects and chemical reactions in human metabolism.[54]

3. RESULTS AND DISCUSSION

3.1. Chemistry and Bioactivity. The strategy adopted for the synthesis of 1,2,3-triazole-8-quinolinol hybrids from 5-azidomethyl-8-quinolinol is outlined in Scheme 1. However, the starting products, such as 5-azidomethyl-8-quinolinol and 5-cyanomethyl-8-quinolinol were synthesized in our laboratory using methods published in our recent work.[24,31] The synthesis of the hybrids follows the proposed mechanism outlined in Scheme 2, which is supported by literature precedent.[55] The reaction of monosubstituted acetonitriles (a) with sodium ethanolate generates the determinate (b), which on in situ treatment with 5-azidomethyl-8-quinolinol (**1**) furnishes selectively the adduct 5-((5-imino-1-alkyl-4,5-dihydro-1*H*-1,2,3-triazol-4-yl)methyl)8-quinolinol (c) via concerted or stepwise [3 + 2]-cycloaddition reaction, which on further rapid isomerization transforms into the 1,2,3-triazole-8-quinolinol hybrids under the reaction conditions.

The 1,2,3-triazole-8-quinolinol hybrids were obtained as white powders with good yields, and their structures were characterized via ^{1}H, ^{13}C NMR, and elemental analysis. The ^{1}H NMR spectra manifested a singlet around 6 ppm, attributed to CH_2 protons situated between the 8-quinolinol and the 1,2,3-triazole rings. A multiplet in the range of 6.9−8.8 ppm corresponds to protons that are aromatic, while -NH_2 protons of 1,2,3-triazole appeared around 7.8 ppm as a singlet. However, the ^{13}C NMR spectra exhibited a signal around 50 ppm, corresponding to the carbon of the methyl group located between the 8-quinolinol and the 1,2,3-triazole rings. The aromatic carbons relating to the 8-quinolinol moiety resonated in the range between 111 and 153 ppm. The appearance of two signals around 108 and 139 ppm exhibited the presence of the quaternary carbons of 1,2,3-triazole, indicating the formation of the 1,2,3-triazole ring.

However, the zone of inhibition (in millimeters) and the MIC values for 1,2,3-triazole-8-quinolinol hybrids toward all bacteria are summarized in Tables 1 and 2. The results obtained were compared with those for nitroxoline, which served as a reference drug.

Inspection of Table 1 exhibited that the hybrids **7**, **8**, and **9** are more active than other hybrids, with inhibition zone diameters of 40, 24, and 19 mm, respectively, at 100 μg/mL against *E. coli*

Table 1. Inhibition Zone Diameter of 1,2,3-Triazole-8-quinolinol Hybrids and Nitroxoline against Various Studied Bacteria[a]

	inhibition zone diameter (mm)			
hybrids	*B. subtilis*	*S. aureus*	*E. coli*	*X. fragariae*
1	-	-	-	-
2	7	8	-	9
3	12	15	10	13
4	11	12	8	12
5	8	7	6	10
6	14	18	12	16
7	31	29	40	34
8	20	23	19	21
9	26	28	24	34
nitroxoline	30	20	32	17
DMSO	-	-	-	-

[a]- means no zone.

Table 2. MICs in μg/mL of 1,2,3-Triazole-8-quinolinol Hybrids

	MICs in μg/mL			
hybrids	*B. subtilis*	*S. aureus*	*E. coli*	*X. fragariae*
2	100	90	100	90
3	60	50	60	50
4	60	60	80	60
5	80	80	90	80
6	40	50	50	30
7	20	10	20	20
8	30	30	40	20
9	20	20	30	10
nitroxoline	20	10	10	10

while hybrids **6**, **3**, and **4** reflected moderate activity against all microorganisms investigated. Hybrids **5** and **2** demonstrated low activity against diverse bacterial strains, while hybrid **1** was inactive. Apparently, hybrids **7** and **9** have comparable antibacterial activity to the reference drug nitroxoline. It is apparent that the antibacterial action of the 1,2,3-triazole-8-quinolinol hybrids is reliant on their molecular structure. Nevertheless, the rise in antibacterial abilities might be explained based on the effects of substituent carried in the C-4 position of the 1,2,3-triazole ring. More so, the presence of electron-donating groups (−Cl, $-C_6H_5$, −8-quinolinol) in the 1,2,3-triazole ring of hybrids **7**, **8**, and **9** can increase biological activity and provide better inhibition while the existence of electron-

https://doi.org/10.1021/acsomega.4c03906
ACS Omega 2024, 9, 25395−25409

Table 3. Calculated Quantum Chemical Variables of 1,2,3-Triazole-8-quinolinol Hybrids

	E_{HOMO}	E_{LUMO}	I	A	ΔE	η	μ	χ	$P\dot{I}$	ω	ε	dipol	energy
						B3LYP/3-21g level							
2	−5.8856	−1.4588	5.8856	1.4588	4.4268	2.2134	0.4518	3.6722	−3.6722	3.0463	0.3283	3.5844	−24487.3150
3	−5.6241	−1.4115	5.6241	1.4115	4.2126	2.1063	0.4748	3.5178	−3.5178	2.9375	0.3404	4.1561	−29220.5553
4	−5.6274	−1.4169	5.6274	1.4169	4.2105	2.1052	0.4750	3.5221	−3.5221	2.9463	0.3394	4.2007	−28157.1101
5	−6.1106	−1.7769	6.1106	1.7769	4.3337	2.1669	0.4615	3.9438	−3.9438	3.5889	0.2786	3.1695	−26120.8935
6	−6.0053	−1.6800	6.0053	1.6800	4.3253	2.1626	0.4624	3.8427	−3.8427	3.4139	0.2929	6.5688	−26555.6274
7	−5.1392	−1.6526	5.1392	1.6526	3.4866	1.7433	0.5736	3.3959	−3.3959	3.3075	0.3023	5.8411	−34867.9240
8	−5.3558	−1.6264	5.3558	1.6264	3.7293	1.8647	0.5363	3.4911	−3.4911	3.2681	0.3060	4.0876	−28241.9673
9	−5.8921	−1.7067	5.8921	1.7067	4.1854	2.0927	0.4778	3.7994	−3.7994	3.4490	0.2899	5.0758	−34437.5625
B3LYP/6-31g level													
2	−6.0570	−1.6112	6.0570	1.6112	4.4458	2.2229	0.4499	3.8341	−3.8341	3.3066	0.3024	2.2526	−24616.0378
3	−5.7917	−1.6847	5.7917	1.6847	4.1070	2.0535	0.4870	3.7382	−3.7382	3.4025	0.2939	4.5457	−29373.7076
4	−5.7993	−1.7119	5.7993	1.7119	4.0875	2.0437	0.4893	3.7556	−3.7556	3.4507	0.2898	4.5476	−28304.7503
5	−6.3313	−1.8928	6.3313	1.8928	4.4385	2.2192	0.4506	4.1121	−4.1121	3.8097	0.2625	7.5886	−26258.2050
6	−6.2747	−1.8395	6.2747	1.8395	4.4352	2.2176	0.4509	4.0571	−4.0571	3.7112	0.2695	7.4080	−26695.2146
7	−5.3479	−1.7810	5.3479	1.7810	3.5669	1.7834	0.5607	3.5644	−3.5644	3.5620	0.2807	5.7015	−35051.5377
8	−5.5332	−1.7307	5.5332	1.7307	3.8025	1.9013	0.5260	3.6319	−3.6319	3.4690	0.2883	4.1562	−28390.7711
9	−6.1384	−1.8267	6.1384	1.8267	4.3117	2.1558	0.4639	3.9826	−3.9826	3.6786	0.2718	5.0496	−34612.5875
B3LYP/SDD level													
2	−6.2549	−1.8977	6.2549	1.8977	4.3571	2.1786	0.4590	4.0763	−4.0763	3.8136	0.2622	2.4264	−24619.2462
3	−5.9830	−1.9307	5.9830	1.9307	4.0524	2.0262	0.4935	3.9568	−3.9568	3.8636	0.2588	4.8577	−29377.9775
4	−5.9917	−1.9726	5.9917	1.9726	4.0192	2.0096	0.4976	3.9821	−3.9821	3.9455	0.2535	7.0385	−28257.4779
5	−6.5368	−2.1775	6.5368	2.1775	4.3593	2.1796	0.4588	4.3571	−4.3571	4.3549	0.2296	7.7989	−26261.8759
6	−6.4769	−2.1198	6.4769	2.1198	4.3571	2.1786	0.4590	4.2983	−4.2983	4.2404	0.2358	7.6160	−26699.1200
7	−5.5691	−2.0686	5.5691	2.0686	3.5005	1.7503	0.5713	3.8189	−3.8189	4.1662	0.2400	5.7153	−35056.0298
8	−5.7365	−2.0079	5.7365	2.0079	3.7285	1.8643	0.5364	3.8722	−3.8722	4.0214	0.2487	4.1579	−28394.1859
9	−6.2851	−2.0977	6.2851	2.0977	4.1873	2.0937	0.4776	4.1914	−4.1914	4.1955	0.2384	4.9331	−34615.4960
HF/3-21g level													
2	−8.3300	2.2074	8.3300	−2.2074	10.5374	5.2687	0.1898	3.0613	−3.0613	0.8894	1.1244	1.9875	−24336.7496
3	−8.0778	2.4597	8.0778	−2.4597	10.5374	5.2687	0.1898	2.8091	−2.8091	0.7488	1.3354	4.8405	−29042.2770
4	−8.0780	2.4594	8.0780	−2.4594	10.5374	5.2687	0.1898	2.8093	−2.8093	0.7490	1.3352	4.8779	−27986.5752
5	−8.5657	1.9511	8.5657	−1.9511	10.5167	5.2584	0.1902	3.3073	−3.3073	1.0401	0.9615	7.5667	−25960.3398
6	−8.5172	1.9952	8.5172	−1.9952	10.5124	5.2562	0.1903	3.2610	−3.2610	1.0116	0.9885	7.4331	−26394.0440
7	−7.5972	2.0561	7.5972	−2.0561	9.6533	4.8267	0.2072	2.7705	−2.7705	0.7952	1.2576	5.4368	−34651.7340
8	−7.7975	2.1211	7.7975	−2.1211	9.9186	4.9593	0.2016	2.8382	−2.8382	0.8121	1.2313	4.3161	−28064.1007
9	−8.5287	1.9903	8.5287	−1.9903	10.5189	5.2595	0.1901	3.2692	−3.2692	1.0160	0.9842	5.1462	−34282.6198
HF/6-31g level													
2	−8.3594	2.0107	8.3594	−2.0107	10.3701	5.1850	0.1929	3.1744	−3.1744	0.9717	1.0291	2.2023	−24463.2759
3	−8.0857	2.2656	8.0857	−2.2656	10.3513	5.1756	0.1932	2.9100	−2.9100	0.8181	1.2224	5.0644	−29192.7729
4	−8.0900	2.2556	8.0900	−2.2556	10.3456	5.1728	0.1933	2.9172	−2.9172	0.8226	1.2157	4.1267	−41460.0701
5	−8.5659	1.7919	8.5659	−1.7919	10.3578	5.1789	0.1931	3.3870	−3.3870	1.1076	0.9029	8.0331	−26095.2850
6	−8.5303	1.8229	8.5303	−1.8229	10.3532	5.1766	0.1932	3.3537	−3.3537	1.0864	0.9205	8.1440	−26531.1870
7	−7.7191	1.7369	7.7191	−1.7369	9.4560	4.7280	0.2115	2.9911	−2.9911	0.9461	1.0569	5.4208	−34832.2905
8	−7.8900	1.9742	7.8900	−1.9742	9.8642	4.9321	0.2028	2.9579	−2.9579	0.8870	1.1274	4.4583	−28210.4814
9	−8.5189	1.8422	8.5189	−1.8422	10.3611	5.1805	0.1930	3.3383	−3.3383	1.0756	0.9297	5.1450	−34455.1882
HF/SDD level													
2	−8.5379	1.6618	8.5379	−1.6618	10.1997	5.0999	0.1961	3.4380	−3.4380	1.1589	0.8629	2.3296	−24466.2988
3	−8.2604	1.9225	8.2604	−1.9225	10.1829	5.0914	0.1964	3.1689	−3.1689	0.9862	1.0140	5.4076	−29196.8142
4	−8.2666	1.9146	8.2666	−1.9146	10.1812	5.0906	0.1964	3.1760	−3.1760	0.9907	1.0093	5.3370	−28135.5770
5	−8.7474	1.4436	8.7474	−1.4436	10.1910	5.0955	0.1963	3.6519	−3.6519	1.3087	0.7641	8.1804	−26098.7496
6	−8.7091	1.4773	8.7091	−1.4773	10.1864	5.0932	0.1963	3.6159	−3.6159	1.2835	0.7791	8.2491	−26534.8159
7	−7.8954	1.5415	7.8954	−1.5415	9.4370	4.7185	0.2119	3.1770	−3.1770	1.0695	0.9350	5.4771	−34836.5314
8	−8.0544	1.6175	8.0544	−1.6175	9.6718	4.8359	0.2068	3.2185	−3.2185	1.0710	0.9337	4.4598	−28213.7644
9	−8.6963	1.4985	8.6963	−1.4985	10.1948	5.0974	0.1962	3.5989	−3.5989	1.2704	0.7871	5.0470	−34457.6997
M062*X*/3-21g level													
2	−7.2919	−0.5358	7.2919	0.5358	6.7561	3.3780	0.2960	3.9138	−3.9138	2.2673	0.4411	1.9800	−24477.1866
3	−7.0753	−0.3325	7.0753	0.3325	6.7428	3.3714	0.2966	3.7039	−3.7039	2.0346	0.4915	4.6438	−29208.1355
4	−7.0731	−0.3274	7.0731	0.3274	6.7458	3.3729	0.2965	3.7002	−3.7002	2.0297	0.4927	4.6986	−28145.2618
5	−7.5812	−0.8729	7.5812	0.8729	6.7082	3.3541	0.2981	4.2270	−4.2270	2.6636	0.3754	7.4427	−26109.9222
6	−7.5020	−0.8142	7.5020	0.8142	6.6878	3.3439	0.2991	4.1581	−4.1581	2.5852	0.3868	7.0258	−29948.5840
7	−6.4625	−0.7940	6.4625	0.7940	5.6684	2.8342	0.3528	3.6283	−3.6283	2.3224	0.4306	6.0365	−34853.7005
8	−6.7387	−0.7206	6.7387	0.7206	6.0181	3.0091	0.3323	3.7296	−3.7296	2.3114	0.4326	5.4287	−28230.2044
9	−7.3564	−0.8283	7.3564	0.8283	6.5281	3.2640	0.3064	4.0924	−4.0924	2.5654	0.3898	5.2944	−34427.7249

https://doi.org/10.1021/acsomega.4c03906
ACS Omega 2024, 9, 25395−25409

Table 3. continued

	E_{HOMO}	E_{LUMO}	I	A	ΔE	η	μ	χ	$P\dot{I}$	ω	ε	dipol	energy
M062X/6-31g level													
2	−7.3888	−0.7116	7.3888	0.7116	6.6772	3.3386	0.2995	4.0502	−4.0502	2.4567	0.4070	2.1100	−24606.4403
3	−7.1215	−0.6378	7.1215	0.6378	6.4837	3.2419	0.3085	3.8797	−3.8797	2.3215	0.4308	4.1250	−29361.9532
4	−7.1186	−0.6642	7.1186	0.6642	6.4543	3.2272	0.3099	3.8914	−3.8914	2.3462	0.4262	4.5572	−28293.5686
5	−7.6818	−0.9946	7.6818	0.9946	6.6873	3.3436	0.2991	4.3382	−4.3382	2.8143	0.3553	7.6907	−26247.7782
6	−7.6301	−0.9508	7.6301	0.9508	6.6794	3.3397	0.2994	4.2905	−4.2905	2.7560	0.3629	7.6137	−26684.7879
7	−6.6470	−0.8974	6.6470	0.8974	5.7495	2.8748	0.3479	3.7722	−3.7722	2.4749	0.4041	5.7541	−35038.0464
8	−6.8647	−0.8256	6.8647	0.8256	6.0391	3.0195	0.3312	3.8451	−3.8451	2.4482	0.4085	4.3347	−28379.5905
9	−7.5708	−0.9364	7.5708	0.9364	6.6345	3.3172	0.3015	4.2536	−4.2536	2.7271	0.3667	5.1252	−34603.1371
M062X/SDD level													
2	−7.6024	−1.0052	7.6024	1.0052	6.5972	3.2986	0.3032	4.3038	−4.3038	2.8077	0.3562	2.2682	−24610.0071
3	−7.3327	−0.8215	7.3327	0.8215	6.5112	3.2556	0.3072	4.0771	−4.0771	2.5530	0.3917	4.2236	−29366.6738
4	−7.3245	−0.8528	7.3245	0.8528	6.4717	3.2359	0.3090	4.0887	−4.0887	2.5831	0.3871	4.3491	−28298.1458
5	−7.8944	−1.2915	7.8944	1.2915	6.6029	3.3014	0.3029	4.5929	−4.5929	3.1948	0.3130	7.8671	−26251.8421
6	−7.8394	−1.2433	7.8394	1.2433	6.5961	3.2980	0.3032	4.5413	−4.5413	3.1267	0.3198	7.7962	−26689.0722
7	−6.8954	−1.1965	6.8954	1.1965	5.6989	2.8495	0.3509	4.0460	−4.0460	2.8724	0.3481	5.7216	−35043.0743
8	−7.0843	−1.1168	7.0843	1.1168	5.9675	2.9838	0.3351	4.1005	−4.1005	2.8176	0.3549	4.3207	−28383.4684
9	−7.7441	−1.2185	7.7441	1.2185	6.5256	3.2628	0.3065	4.4813	−4.4813	3.0775	0.3249	4.9514	−34606.4848

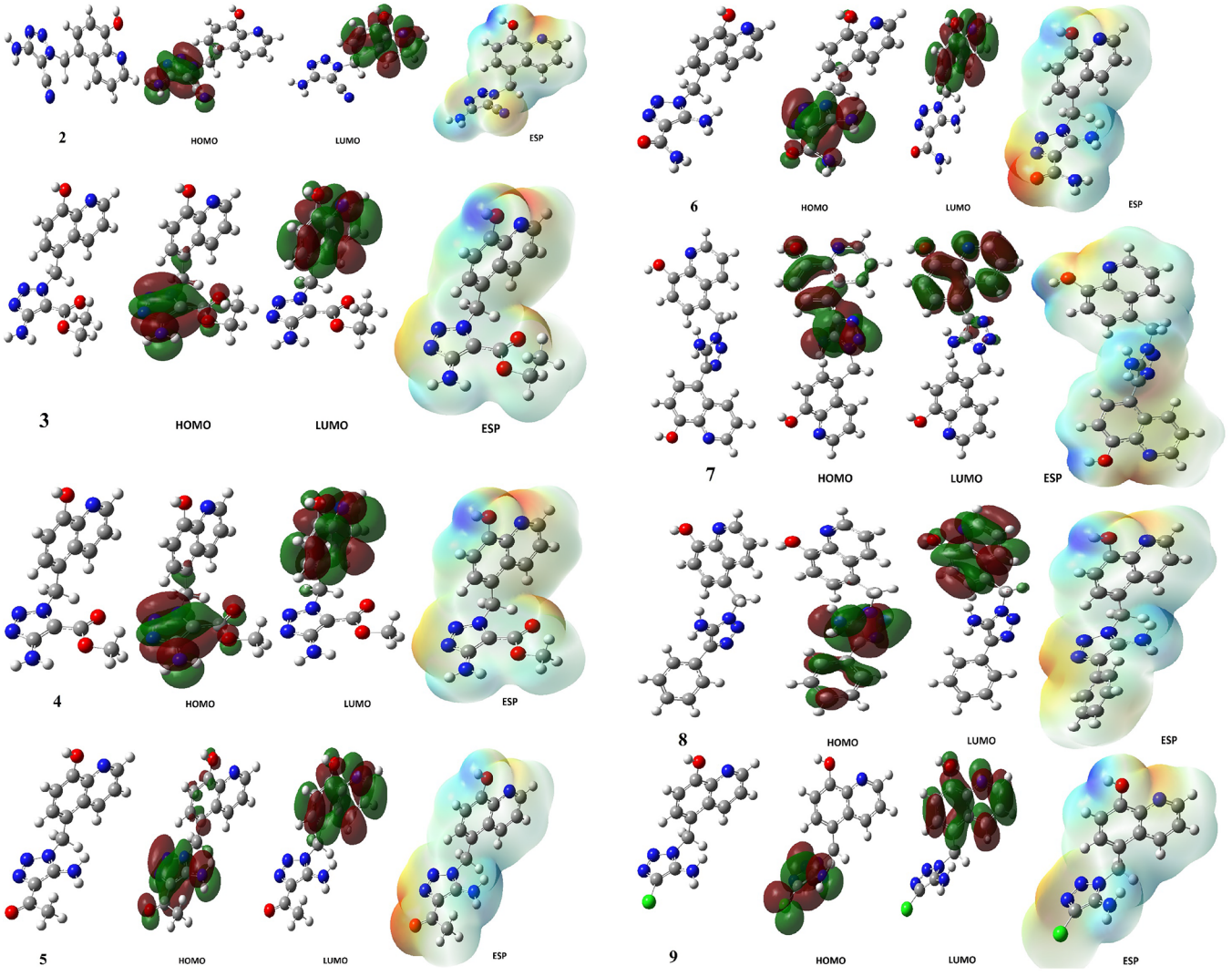

Figure 1. Optimized structure forms, HOMO, LUMO, and electrostatic potential (ESP) of 1,2,3-triazole-8-quinolinol hybrids.

withdrawing groups (−CN, $-COCH_3$) in the 1,2,3-triazole ring of hybrids **2** and **5** decreases biological activity.

Hybrids **7**, **8**, and **9** are the most active compared to other molecules with MIC < 30 mL against all microorganisms, while hybrids **5** and **2** present very limited antibacterial activity (MIC

https://doi.org/10.1021/acsomega.4c03906
ACS Omega 2024, 9, 25395−25409

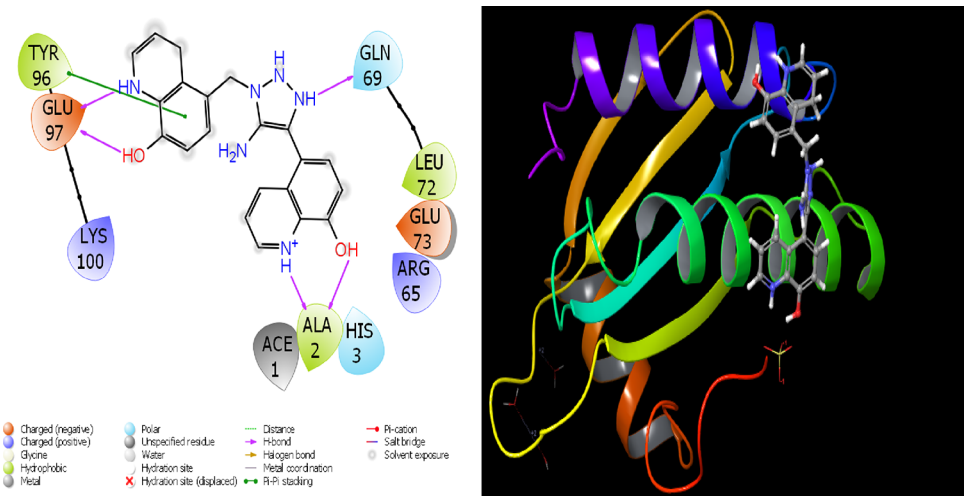

Figure 2. Presentation interactions of hybrid **7** with *B. subtilis*.

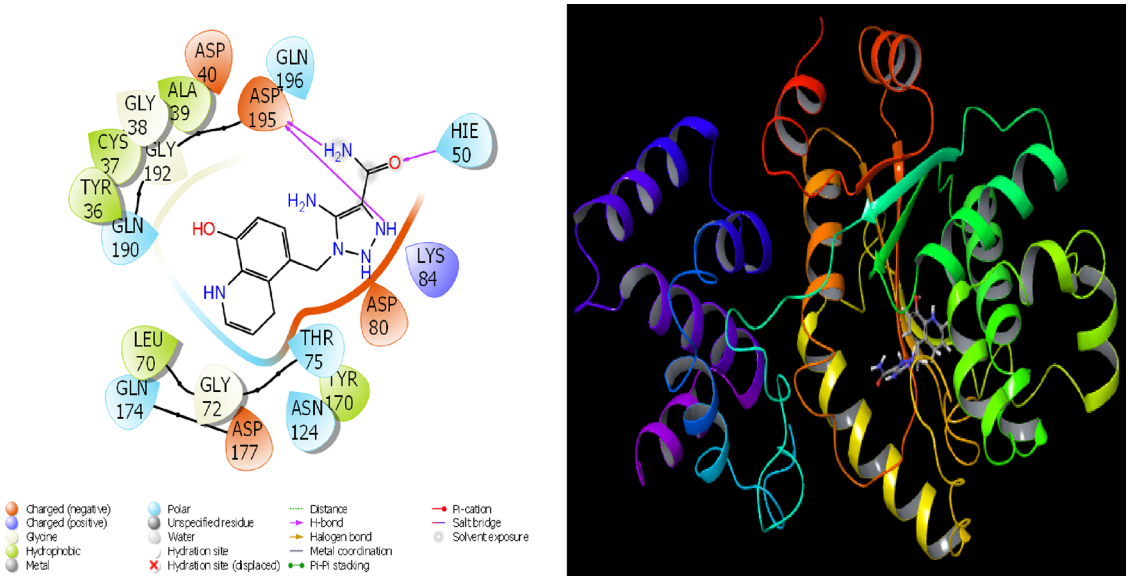

Figure 3. Presentation interactions of hybrid **6** with *S. aureus*.

> 80 μg/mL against all bacteria strains). Whereas hybrid **6** exhibited good to moderate activity with MIC values comprised between 30 μg/mL and 50 μg/mL. Further, hybrids **3** and **4** exhibited moderate activity, with MICs ranging between 50 μg/mL and 70 μg/mL against all strains. These findings reveal that the presence of electron-donating substituents enhances antibacterial abilities, which indicates that biological activity is dependent on molecular structure.

3.2. Theoretical Investigation. Theoretical computations have been undertaken to contrast the chemical and biological characteristics of biomolecules. It offered fundamental preliminary insights prior to the conduct of experimental assays.[47] It offers significant theoretical advantages in discovering active sites in biomolecules and manufacturing better performing and active substances.[48] The two most significant variables in the Gaussian calculations, despite the fact that numerous quantum chemical variables are computed, are HOMO and LUMO, which demonstrate the capacity of molecules for the donation of electrons,[49] and acceptance[48] of them, respectively. However, HOMO, LUMO, and other variables are offered in Table 3.

Table 3 has several variables that have been computed. The ΔE value is one of the variables that demonstrate the activity of 1,2,3-triazole-8-quinolinol hybrids. Broadly, the activity is typically at its greatest when the HOMO variable of a molecule has the most positive value and the LUMO variable has the lowest negative value. Hence, it will be the least among them if the HOMO is the most positive and the LUMO is the most negative. The molecules' activity will rise as a result. The most active molecules are those with the smallest ΔE. The ability of atoms in a molecule to accept bond electrons is indicated by another variable called electronegativity, which is computed.[56] The greater the electronegativity values, the greater the likelihood that the atoms in the molecule will accept bond electrons, lowering the activity of the molecules. A further variable is chemical hardness, which reflects the polarization characteristic of molecules.[49] Chemical softness, on the other hand, is the reverse of chemical hardness. Due to their ease of electron donation, soft molecules are more reactive than hard ones.

Despite the fact that multiple variables have been determined via computational calculations, only a few of these variables have

https://doi.org/10.1021/acsomega.4c03906
ACS Omega 2024, 9, 25395−25409

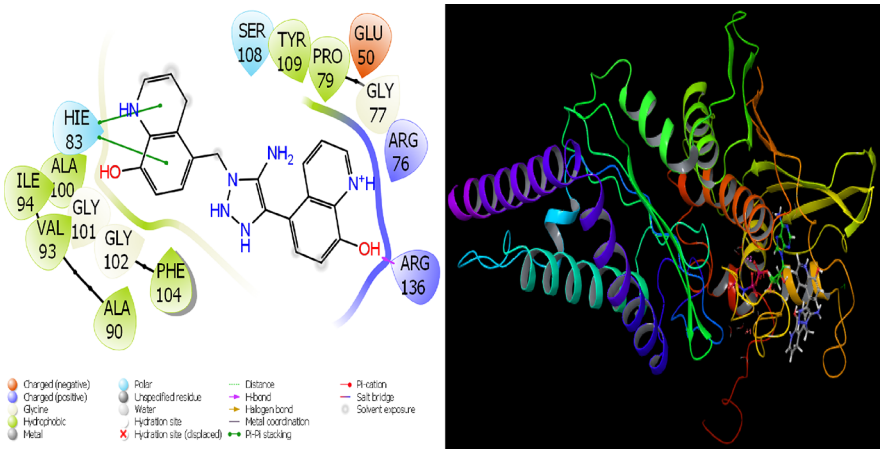

Figure 4. Presentation interactions of hybrid **7** with *E. coli* K-12.

Table 4. Docking Variables Values of 1,2,3-Triazole-8-quinolinol Hybrids against Enzymes

1A6F	Docking Score	Glide ligand efficiency	Glide hbond	Glide evdw	Glide ecoul	Glide emodel	Glide energy	Glide einternal	Glide posenum
2	−3.59	−0.18	−0.41	−10.19	−11.31	−28.24	−21.50	0.66	96
3	−3.42	−0.15	−0.53	−14.41	−11.34	−30.42	−25.75	3.12	132
4	−2.89	−0.13	−0.38	−18.19	−4.68	−27.42	−22.87	0.90	103
5	−3.79	−0.18	−0.43	−12.75	−10.77	−30.30	−23.52	1.62	77
6	−4.27	−0.20	−0.41	−11.66	−14.29	−34.34	−25.95	1.31	67
7	−4.41	−0.15	−0.58	−16.79	−16.94	−42.38	−33.73	3.34	63
8	−4.02	−0.17	−0.38	−14.53	−14.80	−37.77	−29.33	2.58	177
9	−3.61	−0.19	−0.30	−11.03	−11.43	−28.69	−22.46	1.44	81
nitroxoline	−2.84	−0.20	0.00	−9.51	−1.36	−14.40	−10.87	0.12	3
1JIJ	docking Score	Glide ligand efficiency	Glide hbond	Glide evdw	Glide ecoul	Glide emodel	Glide energy	Glide einternal	Glide posenum
2	−6.61	−0.33	−0.05	−39.11	−10.15	−70.13	−49.25	0.08	395
3	−5.97	−0.26	−0.30	−44.54	−7.87	−70.79	−52.41	6.13	301
4	−7.04	−0.32	−0.41	−46.87	−9.99	−80.16	−56.86	2.55	288
5	−6.13	−0.29	−0.09	−41.35	−7.80	−65.67	−49.16	1.10	248
6	−7.26	−0.35	−0.67	−34.69	−14.32	−71.93	−49.01	3.96	334
7	−7.02	−0.24	−0.71	−39.69	−17.83	−91.89	−57.52	3.21	316
8	−6.25	−0.26	−0.66	−39.10	−8.62	−67.96	−47.73	1.96	353
9	−6.64	−0.35	−0.41	−33.38	−12.47	−63.71	−45.86	0.75	316
nitroxoline	−6.14	−0.44	−0.40	−27.82	−0.31	−39.59	−28.13	0.03	238
4WUB	docking Score	Glide ligand efficiency	Glide hbond	Glide evdw	Glide ecoul	Glide emodel	Glide energy	Glide einternal	Glide posenum
2	−4.94	−0.25	−0.61	−20.83	−11.66	−43.80	−32.49	1.94	108
3	−4.57	−0.20	−0.06	−34.23	−3.05	−48.86	−37.29	1.19	149
4	−4.28	−0.19	−0.33	−30.40	−4.97	−46.08	−35.37	0.64	286
5	−4.99	−0.24	−0.18	−31.87	−4.18	−47.69	−36.06	1.07	6
6	−5.07	−0.24	−0.18	−32.16	−5.19	−50.65	−37.36	0.80	340
7	−6.28	−0.22	−0.48	−32.78	−13.29	−66.09	−46.08	2.30	171
8	−5.23	−0.22	−0.32	−31.33	−6.98	−49.99	−38.31	3.79	274
9	−5.54	−0.29	−0.61	−25.07	−4.00	−39.04	−29.07	2.31	210
nitroxoline	−4.58	−0.33	−0.27	−19.05	−1.69	−28.12	−20.74	0.12	315

figural representations. Nevertheless, optimal forms of the initial visual molecules are displayed in Figure 1. The second and third images correspond to HOMO and LUMO, respectively. While the electrostatic potentials of the structures are displayed in the final image, On the visual molecule, there are red-colored zones that are electron-rich. On the visual molecule, there are blue-colored zones that are deficient in electrons. Both of these zones are the molecule's centers of activity for accepting and donating electrons.[47,48] According to Gaussian calculations, hybrid **7** exhibited greater biological activity than its counterparts in computations made at the B3LYP, HF, and M062X levels.

After the Gaussian computations, through which the actions of 1,2,3-triazole-8-quinolinol hybrids toward biological microorganisms were scrutinized. The 1,2,3-triazole-8-quinolinol hybrids' activities toward several bacterial proteins were assessed. The chemical interaction that happens among 1,2,3-triazole-8-quinolinol hybrids and proteins is considered to be an essential factor in determining molecular activity. These chemical interactions include bonds of hydrogen, polarity, hydrophobic interactions, $\pi-\pi$, and halogen.[33,41] Figures 2−4 depict the interactions of the proteins and 1,2,3-triazole-8-quinolinol hybrids. Table 4 illustrates the variables derived from these interactions.

https://doi.org/10.1021/acsomega.4c03906
ACS Omega 2024, 9, 25395−25409

Table 5. ADME/T Properties of Hybrids

	2	3	4	5	6	7	8	9	reference range
mol_MW	270	317	303	287	288	388	321	280	130−725
dipole (D)	8.7	5.7	5.9	4.0	3.2	4.4	2.1	2.7	1.0−12.5
SASA	489	542	521	514	503	661	581	479	300−1000
FOSA	45	172	133	123	48	48	48	48	0−750
FISA	261	200	217	219	282	250	171	180	7−330
PISA	184	171	171	173	173	363	362	177	0−450
WPSA	0	0	0	0	0	0	0	74	0−175
volume (A^3)	837	964	914	891	867	1170	1018	818	500−2000
donorHB	6	3	3	4	6	7	6	6	0−6
accptHB	3.8	1.3	1.3	2.3	2.8	4.0	2.3	2.3	2.0−20.0
glob (Sphere = 1)	0.9	0.9	0.9	0.9	0.9	0.8	0.8	0.9	0.75−0.95
QPpolrz (A^3)	25.9	30.2	28.8	28.0	27.0	40.9	35.5	25.7	13.0−70.0
QPlogPC16	10.5	10.5	10.2	10.2	10.9	15.0	12.8	10.3	4.0−18.0
QPlogPoct	20.8	15.5	15.2	16.6	19.7	26.8	22.0	18.8	8.0−35.0
QPlogPw	15.3	7.8	8.1	10.6	14.4	18.6	14.9	13.4	4.0−45.0
QPlogPo/w	0.4	3.1	2.6	1.9	0.7	2.3	2.7	1.5	−2.0−6.5
QPlogS	−3.2	−4.1	−3.8	−3.2	−2.4	−4.6	−3.9	−2.5	−6.5−0.5
CIQPlogS	−4.5	−5.6	−5.3	−4.5	−4.1	−6.1	−5.2	−4.1	−6.5−0.5
QPlogHERG	−4.4	−4.4	−4.4	−4.4	−4.4	−6.3	−5.8	−4.3	[a]
QPPCaco (nm/sec)	33	126	86	84	21	42	237	194	[b]
QPlogBB	−2.0	−1.6	−1.6	−1.7	−2.2	−2.3	−1.3	−1.0	−3.0−1.2
QPPMDCK (nm/sec)	13	53	35	34	8	16	105	212	[b]
QPlogKp	−5.2	−4.0	−4.4	−4.5	−5.6	−4.4	−3.0	−3.8	Kp in cm/h
IP (ev)	7.3	7.1	7.1	7.2	7.2	7.1	6.9	7.1	7.9−10.5
EA (eV)	−0.1	0.1	0.1	0.1	0.2	0.8	−0.2	−0.2	−0.9−1.7
#metab	6	6	6	6	7	7	6	6	1−8
QPlogKhsa	−0.5	0.4	0.3	0.0	−0.3	0.1	0.1	−0.4	−1.5−1.5
Human Oral Absorption	2	3	3	2	2	2	3	3	
Percent Human Oral Absorption	43	70	64	59	41	57	72	64	[c]
PSA	122	125	128	121	148	125	94	95	7−200
RuleOfFive	1.0	1.0	1.0	1.0	1.0	1.0	1.0	1.0	maximum is 4
RuleOfThree	0.0	0.0	0.0	0.0	2.0	1.0	0.0	0.0	maximum is 3
Jm	0.0	0.0	0.0	0.0	0.0	0.0	0.0	0.1	

[a]Concern below −5. [b]<25 is poor and >500 is great. [c]<25% is poor and >80% is high.

As an outcome of the molecular docking calculations, the interactions of the 1,2,3-triazole-8-quinolinol hybrids were determined. Table 4 summarizes the most significant variables collected following the procedure. These variables quantify the chemical interactions (Glide hbond, Glide evdw, and Glide ecoul) that occur between 1,2,3-triazole-8-quinolinol hybrids and proteins.[33] However, numerical data can be generated about the poses (Glide emodel, Glide energy, Glide einternal, and Glide posenum) acquired from the interaction of 1,2,3-triazole-8-quinolinol hybrids with proteins.[41]

As a result of the calculations, when the interaction of the hybrid **7** molecule with *B. subtilis* is examined in Figure 2, it is seen that the hydroxy group and amine group in the 1,4-dihydroquinolin-8-ol ring on the left side of the molecule make hydrogen bonds with the GLU 97 protein. It is observed that the same ring forms a $\pi-\pi$ stacking interaction with the TYR 96 protein. At the same time, the hydroxy and amine groups in the 1,4-dihydroquinolin-8-ol ring on the right side of the molecule appear to hydrogen bond with the ALA 2 protein.

In Figure 3, it is seen that in the interaction of the hybrid **6** molecule with the *S. aureus* protein, the nitrogen atom in the triazole ring in the hybrid **6** molecule and the amine group attached to the carbonyl carbon make a hydrogen bond with the ASP 195 protein.

When the interaction between the hybrid **7** molecule and the *E. coli* K-12 protein is examined in Figure 4, it is seen that the 1,4-dihydroquinolin-8-ol ring creates a $\pi-\pi$ stacking interaction with the HIE protein.

The findings of molecular docking alone are insufficient since they compare the theoretical activities of hybrids but do not propose their usage as a medication. As a result, ADME/T analysis is done to forecast the motions of molecules in human metabolism and to investigate their impact and responses in human metabolism.[57] The chemical and biological characteristics of hybrids were assessed and summarized in Table 5. A number of variables were determined, comprising the molar mass of 1,2,3-triazole-8-quinolinol hybrids (mol_MW), the dipole moment (dipole), the total solvent accessible surface area (SASA), the volume, the accptHB (accepted hydrogen bond), the globularity descriptor (glob), the predicted polarizability (QPpolrz), the donorHB (provided hydrogen bond), and the globularity descriptor (glob).[58] In addition, in order to inquire about the biological features of 1,2,3-triazole-8-quinolinol hybrids, their movements in human metabolism have been hypothesized. For this, many variables were computed, including brain-blood (QPPMDCK), intestinal-blood (QPPCaco) molecular barriers, the number of probable metabolic reactions (#metab), and predicted skin permeability (QPlogKp).[59] Aside from the aforementioned variables,

https://doi.org/10.1021/acsomega.4c03906
ACS Omega 2024, 9, 25395−25409

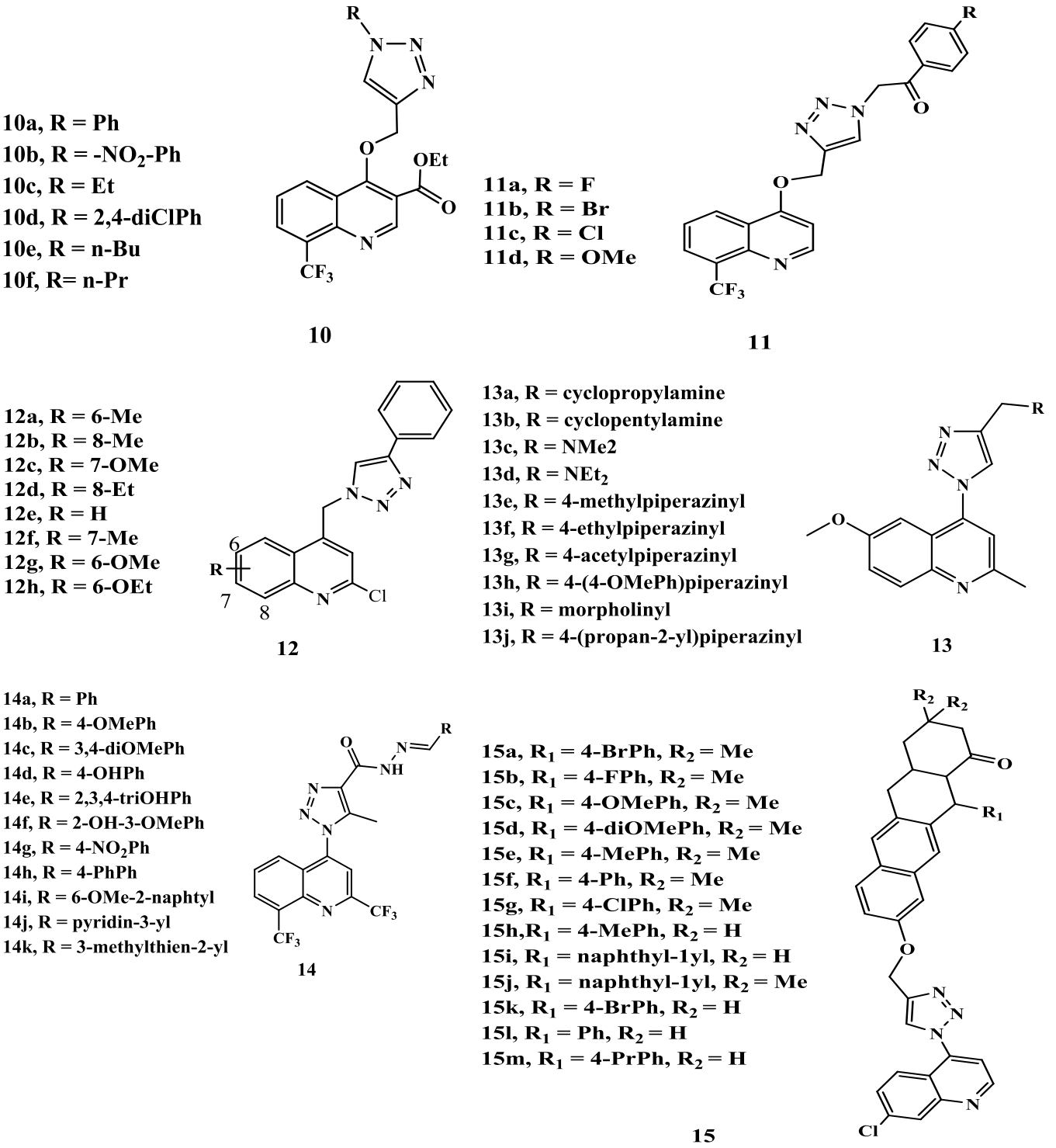

Figure 5. Chemical structures of 1,2,3-triazole-quinoline hybrids **10**−**15**.

violations of Lipinski's rule of five (Rule of Five)[60,61] and violations of Jorgensen's rule of three (Rule of Three)[62] are essential variables. This essential variable must have a numerical value of zero. When the numerical values of all calculated variables were checked, it was found that there was no harm in applying all chemicals to human metabolism as a theoretical medicine.

3.3. Comparative Study. Several studies have investigated the antibacterial properties of various 1,2,3-triazole-quinoline hybrids (Figure 5). Hybrids **12** showed promising in vitro activity against *B. subtilis* and *E. coli*, with MIC values ranging from 10 to 25 μg/mL.[63] Similarly, ether-linked 8-trifluoromethylquinoline-1,2,3-triazole hybrids **10** and **11** exhibited weak to moderate antibacterial activities against *E. coli*, *B. subtilis*, and *P. aeruginosa*, with inhibition zones ranging from 2 to 16 mm at 1 μg/mL, albeit less potent than ciprofloxacin (inhibition zone: 24−28 mm at 1 μg/mL).[64] Thomas et al. evaluated the in vitro antimicrobial activities of 1,2,3-triazole-quinoline hybrids **13** against a panel of Gram-positive and Gram-negative bacteria, showing moderate to excellent activities with MICs of 6.25−50

https://doi.org/10.1021/acsomega.4c03906
ACS Omega 2024, 9, 25395−25409

μg/mL.[65] However, introducing hydrazone into the 1,2,3-triazole motif,[66] as seen in hybrids **14**, did not enhance the antibacterial activities (MIC: 6.25−25 μg/mL) compared to analogs **13**. Quinoline-1,2,3-triazole-xanthene hybrids **15** displayed moderate antibacterial activities against *S. aureus*, *S. pyogenes*, and *B. cereus*, with MIC values ranging from 16 to 128 μg/mL.[67] Finally, the hybrids presented in our study exhibited moderate to excellent activities (especially hybrid **7**), with MIC values ranging from 10 to 100 μg/mL, against *S. aureus*, *E. coli*, *B. subtilis*, and *X. fragariae*, showcasing their potential compared to other hybrids with similar structures mentioned in the literature.

3.4. Structure−Activity Relationship. The SARs study in this investigation demonstrated that 5-(5-amino-1-((8-quinolinol-5-yl)methyl)-1*H*-1,2,3-triazol-4-yl) 8-quinolinol (**7**) showed excellent activity against all four bacterial pathogens, i.e., Gram-positive as well as Gram-negative bacteria, due to the presence of an aromatic heterocyclic group (8-quinolinol) in the molecule. Hybrids having electron-withdrawing substituents (−$CONH_2$, −CO_2Et, −CO_2Me, −COMe, −CN (−M effect)) demonstrated less or moderate activity, and hybrids containing electron-donating substituents (−C_6H_5, −Cl (+M effect)) showed good activity against all the tested strains, viz., *S. aureus*, *B. subtilis*, *E. coli*, and *X. fragariae*. The presence of an electron-withdrawing group (−M effect) on the 1,2,3-triazole ring at the 4-position led to a decrease in the antimicrobial activity of these molecules, and the trends in the order of activity with respect to electron-withdrawing substituents were found to be $CONH_2$ > CO_2Et > CO_2Me > COMe > CN. The above observation indicated that the antimicrobial activity of the synthesized hybrids decreases with the increase in the electron-withdrawing power of the substituents present in the 1,2,3-triazole ring at the 4-position.[68,69] This evidence confirmed that suitable functional groups on the 1,2,3-triazole ring at the 4-position were essential for better antimicrobial activities in drug design. Remarkably, the electron-donating groups (−C_6H_5, -Cl) on the 1,2,3-triazole ring showed good activity due to an increase in the electron-donating power. Hence, these results implied that the electron-donating groups play an important role in increasing the antimicrobial activity of synthesized hybrids. However, the lack of antibacterial activity observed with hybrid **1** indicates that the presence of the 1,2,3-triazole ring is essential for eliciting antibacterial effects.

4. CONCLUSIONS

In summary, eight new 1,2,3-triazole-8-quinolinol hybrids were synthesized from monosubstituted acetonitriles and 5-azidomethyl-8-quinolinol in good yield by a single-step reaction. All hybrid structures (**2**−**9**) were identified by analytical and spectral methods and screened in vitro for antimicrobial evaluation against four bacterial strains (*Escherichia coli*, *Xanthomonas fragariae*, *Staphylococcus aureus*, and *Bacillus subtilis*). The preliminary studies revealed that some of the hybrids exhibited comparable bioactivities to the reference drugs. The activity of 1,2,3-triazole-8-quinolinol hybrids was found to be significantly enhanced when incorporating an electron-donating substituent on the 1,2,3-triazole ring at the 4-position, in contrast to electron-withdrawing substituents at the same position. The hybrid **7** exhibited antibacterial activity (MIC = 10 μg/mL against *S. aureus* bacteria) comparable with nitroxoline (MIC = 10 μg/mL). In this study, first, three different basis sets were selected at three different levels. Three different basis sets were selected at each level for the 8 molecules in the study, and how these basis sets changed the quantum chemical parameters of the molecules was examined. Additionally, molecular modeling studies indicated that the hybrid **7** binds effectively with the active sites of the enzymes (DNA gyrase) via hydrogen bonding, hydrophobic interaction, and electrostatic interactions. The present work provides hybrid **7** as a promising lead that could be used for the development of new antimicrobial agents.

ASSOCIATED CONTENT

Supporting Information

The Supporting Information is available free of charge at https://pubs.acs.org/doi/10.1021/acsomega.4c03906.

Copies of ^{1}H and ^{13}C NMR spectra of all new 1,2,3-triazole-8-quinolinol hybrids (PDF)

AUTHOR INFORMATION

Corresponding Author

Abdelkader Zarrouk − *Laboratory of Materials, Nanotechnology, and Environment, Department of Chemistry, Faculty of Sciences, Mohammed V University in Rabat, Rabat 10500, Morocco; Research Centre, Manchester Salt & Catalysis, Manchester M15 4AN, United Kingdom;* orcid.org/0000-0002-5495-2125; Phone: 00212665201397; Email: azarrouk@gmail.com

Authors

Mohamed El Faydy − *Laboratory of Organic Chemistry, Catalysis, and Environment, Department of Chemistry, Faculty of Sciences, Ibn Tofaïl University, Kenitra 14000, Morocco*

Loubna Lakhrissi − *Laboratory of Organic Chemistry, Catalysis, and Environment, Department of Chemistry, Faculty of Sciences, Ibn Tofaïl University, Kenitra 14000, Morocco; Laboratory of Heterocyclic Organic Chemistry, Faculty of Sciences, Mohammed V University, Rabat 10500, Morocco*

Naoufel Dahaieh − *Laboratory of Nutrition, Health, and Environment, Department of Biology, Faculty of Sciences, Ibn Tofaïl University, Kenitra 14000, Morocco*

Khadija Ounine − *Laboratory of Nutrition, Health, and Environment, Department of Biology, Faculty of Sciences, Ibn Tofaïl University, Kenitra 14000, Morocco*

Burak Tüzün − *Plant and Animal Production Department, Technical Sciences Vocational School of Sivas, Sivas Cumhuriyet University, Sivas 58140, Turkey;* orcid.org/0000-0002-0420-2043

Nabila Chahboun − *Laboratory of Natural Resources and Sustainable Development, Faculty of Sciences, Ibn Tofail University, Kenitra 14000, Morocco; Institute of Nursing Professions and Health Techniques, Kenitra 14000, Morocco; Laboratory of Materials, Nanotechnology, and Environment, Department of Chemistry, Faculty of Sciences, Mohammed V University in Rabat, Rabat 10500, Morocco*

Ahmed Boshaala − *Libyan Authority for Scientific Research, Tripoli, Libya; Research Centre, Manchester Salt & Catalysis, Manchester M15 4AN, United Kingdom*

Abeer AlObaid − *Department of Chemistry, College of Science, King Saud University, Riyadh 11451, Saudi Arabia*

Ismail Warad − *Research Centre, Manchester Salt & Catalysis, Manchester M15 4AN, United Kingdom; Department of Chemistry, AN-Najah National University, Nablus 00970, Palestine;* orcid.org/0000-0001-8853-8961

https://doi.org/10.1021/acsomega.4c03906
ACS Omega 2024, 9, 25395−25409

Brahim Lakhrissi − *Laboratory of Organic Chemistry, Catalysis, and Environment, Department of Chemistry, Faculty of Sciences, Ibn Tofaïl University, Kenitra 14000, Morocco*

Complete contact information is available at: https://pubs.acs.org/10.1021/acsomega.4c03906

Notes

The authors declare no competing financial interest.

■ ACKNOWLEDGMENTS

The authors extend their appreciation to the Researchers Supporting Project number (RSP2024R381), King Saud University, Riyadh, Saudi Arabia. The authors would like to thank the National Centre for Scientific and Technical Research (CNRST) of Morocco for putting at their disposal the technical facilities of the UATRS Division

■ REFERENCES

(1) Furst, A. L.; Francis, M. B. Impedance-based detection of bacteria. *Chem. Rev.* **2019**, *119*, 700−726.
(2) Bonandi, E.; Christodoulou, M. S.; Fumagalli, G.; Perdicchia, D.; Rastelli, G.; Passarella, D. The 1,2,3-triazole ring as a bioisostere in medicinal chemistry. *Drug Discovery Today.* **2017**, *22*, 1572−1581.
(3) Zhang, S.; Xu, Z.; Gao, C.; Ren, Q. C.; Chang, L.; Lv, Z. S.; Feng, L. S. Triazole derivatives and their anti-tubercular activity. *Eur. J. Med. Chem.* **2017**, *138*, 501−513.
(4) Labadie, G. R.; de la Iglesia, A.; Morbidoni, H. R. Targeting tuberculosis through a small focused library of 1,2,3-triazoles. *Mol. Divers.* **2011**, *15*, 1017−1024.
(5) Boechat, N.; Ferreira, V. F.; Ferreira, S. B.; Ferreira, M. de L. G.; da Silva, F. de C.; Basto, M. M.; Costa, M. D. S.; Loureno, M. C. S.; Pinto, A. C.; Krettli, A. U.; Aguiar, A. C.; Teixeira, B. M.; da Silva, N. V.; Martins, P. R. C.; Bezerra, F. A. F. M.; Camilo, A. L. S.; da Silva, G. P.; Costa, C. C. P. Novel 1,2,3-triazole derivatives for use against Mycobacterium tuberculosis H37Rv (ATCC 27294) strain. *J. Med. Chem.* **2011**, *54*, 5988−5999.
(6) Shanmugavelan, P.; Nagarajan, S.; Sathishkumar, M.; Ponnuswamy, A.; Yogeeswari, P.; Sriram, D. Efficient synthesis and in vitro antitubercular activity of 1,2,3-triazoles as inhibitors of Mycobacterium tuberculosis. *Bioorg. Med. Chem. Lett.* **2011**, *21*, 7273−7276.
(7) Gill, C.; Jadhav, G.; Shaikh, M.; Kale, R.; Ghawalkar, A.; Nagargoje, D.; Shiradkar, M. Clubbed [1,2,3]triazoles by fluorine benzimidazole: a novel approach to H37Rv inhibitors as a potential treatment for tuberculosis. *Bioorg. Med. Chem. Lett.* **2008**, *18*, 6244−6247.
(8) Tripathi, R. P.; Yadav, A. K.; Ajay, A.; Bisht, S. S.; Chaturvedi, V.; Sinha, S. K. Application of Huisgen (3 + 2) cycloaddition reaction: synthesis of 1-(2,3-dihydrobenzofuran-2-yl-methyl [1,2,3]-triazoles and their antitubercular evaluations. *Eur. J. Med. Chem.* **2010**, *45*, 142−148.
(9) Gadhave, P. P.; Dighe, N. S.; Pattan, S. R.; Deotarse, P.; Musmade, D. S.; Shete, R. V. Current biological and synthetic profile of triazoles: a review. *Ann. Biol. Res.* **2010**, *1*, 82−89.
(10) Dheer, D.; Singh, V.; Shankar, R. Medicinal attributes of 1,2,3-triazoles: current developments. *Bioorg. Chem.* **2017**, *71*, 30−54.
(11) Saravolatz, L. D.; Johnson, L. B.; Kauffman, C. A. Voriconazole: a new triazole antigungal agent. *Clin. Infect. Dis.* **2003**, *36*, 630−637.
(12) Xu, J. H.; Fan, Y. L.; Zhou, J. Quinolone-triazole hybrids and their biological activities. *J. Heterocycl. Chem.* **2018**, *55*, 1854−1862.
(13) Gao, F.; Zhang, X.; Wang, T.; Xiao, J. Quinolone hybrids and their anti-cancer activities: an overview. *Eur. J. Med. Chem.* **2019**, *165*, 59−79.
(14) Eswaran, S.; Adhikari, A. V.; Shetty, N. S. Synthesis and antimicrobial activities of novel quinoline derivatives carrying 1,2,4-triazole moiety. *Eur. J. Med. Chem.* **2009**, *44*, 4367−4647.
(15) Fan, Y.-L.; Ke, X.; Li, M. Coumarin-triazole hybrids and their biological activities. *J. Heterocycl. Chem.* **2018**, *55*, 791−80.
(16) Gao, C.; Chang, L.; Xu, Z.; Yan, X. F.; Ding, C.; Zhao, F.; Wu, X.; Feng, L. S. Recent advances of tetrazoles as potential anti-tubercular and anti-malarial agents. *Eur. J. Med. Chem.* **2019**, *163*, 404−412.
(17) Meunier, B. Hybrid molecules with a dual mode of action: dream or reality? *Acc. Chem. Res.* **2008**, *41*, 69−77.
(18) Mishra, S. S.; Singh, P. Hybrids molecules: the privileged scaffolds for various pharmaceuticals. *Eur. J. Med. Chem.* **2016**, *124*, 500−536.
(19) Gao, F.; Zhang, X.; Wang, T.; Xiao, J. Quinolone hybrids and their anti-cancer activities: an overview. *Eur. J. Med. Chem.* **2019**, *165*, 59−79.
(20) Xu, Z.; Zhao, S.; Lv, Z.; Feng, L.; Wang, Y.; Zhang, F.; Bai, L.; Deng, J. Benzofuran derivatives and their anti-tubercular, anti-bacterial activities. *Eur. J. Med. Chem.* **2019**, *162*, 266−276.
(21) Xu, Z.; Gao, C.; Ren, Q. C.; Song, X. F.; Feng, L. S.; Lv, Z. S. Recent advances of pyrazole- containing derivatives as anti-tubercular agents. *Eur. J. Med. Chem.* **2017**, *139*, 429−440.
(22) Hu, Y. Q.; Gao, C.; Zhang, S.; Xu, L.; Xu, Z.; Feng, L. S.; Wu, X.; Zhao, F. Quinoline hybrids and their antiplasmodial and antimalarial activities. *Eur. J. Med. Chem.* **2017**, *139*, 22−47.
(23) Mahmoud, M. E.; Mohamed, A. K. Efficient removal of La (III) from water by surface metal sequestration methodology using 5-azo-phenolate-8-hydroxyquinoline as a task designed sequestering material. *J. Ind. Eng. Chem.* **2018**, *63*, 220−229.
(24) El Faydy, M.; Lakhrissi, B.; Jama, C.; Zarrouk, A.; Olasunkanmi, L. O.; Ebenso, E. E.; Bentiss, F. Electrochemical, surface and computational studies on the inhibition performance of some newly synthesized 8-hydroxyquinoline derivatives containing benzimidazole moiety against the corrosion of carbon steel in phosphoric acid environment. *J. Mater. Res. Technol.* **2020**, *9*, 727−748.
(25) Velthuisen, E. J.; Johns, B. A.; Temelkoff, D. P.; Brown, K. W.; Danehower, S. C. The design of 8-hydroxyquinoline tetracyclic lactams as HIV-1 integrase strand transfer inhibitors. *Eur. J. Med. Chem.* **2016**, *117*, 99−112.
(26) Zhang, H. R.; Meng, T.; Liu, Y. C.; Chen, Z. F.; Liu, Y. N.; Liang, H. Synthesis, characterization, and biological evaluation of a cobalt (II) complex with 5-chloro-8-hydroxyquinoline as anticancer agent. *Appl. Organomet. Chem.* **2016**, *30*, 740−747.
(27) Nehra, N.; Tittal, R. K.; Ghule, V. D. 1,2,3-Triazoles of 8-Hydroxyquinoline and HBT: Synthesis and Studies (DNA Binding, Antimicrobial, Molecular Docking, ADME, and DFT). *ACS omega* **2021**, *6*, 4127089−27100.
(28) El Faydy, M.; Dahaieh, N.; Ounine, K.; Rastija, V.; Almalki, F.; Jamalis, J.; Zarrouk, A.; Hadda, T. B.; Lakhrissi, B. Synthesis and antimicrobial activity evaluation of some new 7-substituted quinolin-8-ol derivatives: POM analyses, docking, and identification of antibacterial pharmacophore sites. *Chem. Data Collect.* **2021**, *31*, No. 100593.
(29) El Faydy, M.; Djassinra, T.; Haida, S.; Rbaa, M.; Ounine, K.; Kribii, A.; Lakhrissi, B. Synthesis and investigation of antibacterial and antioxidants properties of some new 5-subsituted- 8-hydroxyquinoline derivatives. *J. Mater. Environ. Sci.* **2017**, *8*, 3855−3863.
(30) Abdel-Mohsen, S. A. Heterocycles derived from 5-(2-amino-tiazol-4-yl)-8-hydroxyquinoline: synthesis and antimicrobial activity. *J. Chin. Chem. Soc.* **2003**, *50*, 1085−1092.
(31) El Faydy, M.; Dahaieh, N.; Ounine, K.; Lakhrissi, B.; Warad, I.; Tüzün, B.; Zarrouk, A. Synthesis, Identification, Antibacterial Activity, ADME/T and 1BNA-Docking Investigations of 8-Quinolinol Analogs Bearing a Benzimidazole Moiety. *Arabian J. Sci. Eng.* **2022**, *47*, 497−510.
(32) Abbout, S.; Hsissou, R.; Erramli, H.; Chebabe, D.; Salim, R.; Kaya, S.; Hajjaji, N. Gravimetric, electrochemical and theoretical study, and surface analysis of novel epoxy resin as corrosion inhibitor of carbon steel in 0.5 M H2SO4 solution. *J. Mol. Struct.* **2021**, *1245*, No. 131014.
(33) Koçyiğit, Ü. M.; Doğan, M.; Muğlu, H.; Taslimi, P.; Tüzün, B.; Yakan, H.; Bal, H.; Güzel, E.; Gülçin, İ. Determination of biological

studies and molecular docking calculations of isatin-thiosemicarbazone hybrid compounds. *J. Mol. Struct.* **2022**, *1264*, No. 133249.
(34) El-Gammal, O. A.; El-Bindary, A. A.; Mohamed, F. S.; Rezk, G. N.; El-Bindary, M. A. Synthesis, characterization, design, molecular docking, anti COVID-19 activity, DFT calculations of novel Schiff base with some transition metal complexes. *J. Mol. Liq.* **2022**, *346*, No. 117850.
(35) Abou-Melha, K. S.; Al-Hazmi, G. A.; Althagafi, I.; Alharbi, A.; Shaaban, F.; El-Metwaly, N. M.; El-Bindary, A. A.; El-Bindary, M. A. Synthesis, characterization, DFT calculation, DNA binding and antimicrobial activities of metal complexes of dimedone arylhydrazone. *J. Mol. Liq.* **2021**, *334*, No. 116498.
(36) Becke, A. D. Density-functional thermochemistry. I. The effect of the exchange-only gradient correction. *J. Chem. Phys.* **1992**, *96*, 2155−2160.
(37) Vautherin, D.; Brink, D. T. Hartree-Fock calculations with Skyrme's interaction. I. Spherical nuclei. *Phys. Rev.* **1972**, *C5*, 626.
(38) Hohenstein, E. G.; Chill, S. T.; Sherrill, C. D. Assessment of the performance of the M05− 2X and M06− 2X exchange-correlation functionals for noncovalent interactions in biomolecules. *J. Chem. Theory Comput.* **2008**, *4*, 1996−2000.
(39) Qiu, X.; Janson, C. A.; Smith, W. W.; Green, S. M.; McDevitt, P.; Johanson, K.; Carter, P.; Hibbs, M.; Lewis, C.; Chalker, A.; Fosberry, A.; Lalonde, J.; Berge, J.; Brown, P.; Houge-Frydrych, C. S.; Jarvest, R. L. Crystal structure of Staphylococcus aureus tyrosyl-tRNA synthetase in complex with a class of potent and specific inhibitors. *Protein Sci.* **2001**, *10*, 2008−2016.
(40) Hearnshaw, S. J.; Chung, T. H.; Stevenson, C. E. M.; Maxwell, A.; Lawson, D. M. The role of monovalent cations in the ATPase reaction of DNA gyrase. *Acta Crystallogr., Sect. D: Biol. Crystallogr.* **2015**, *71*, 996−1005.
(41) Erdogan, M. K.; Gundogdu, R.; Yapar, Y.; Gecibesler, I. H.; Kirici, M.; Behcet, L.; Tuzun, B.; Taslimi, P. The Evaluation of Anticancer, Antioxidant, Antidiabetic and Anticholinergic Potentials of Endemic Rhabdosciadium microcalycinum Supported by Molecular Docking Study. *ChemistrySelect* **2022**, *7*, No. e202200400.
(42) Hsissou, R.; Benhiba, F.; Echihi, S.; Benzidia, B.; Cherrouf, S.; Haldhar, R.; Ahmad Alvi, P.; Kaya, S.; Serdaroğlu, G.; Zarrouk, A. Performance of curing epoxy resin as potential anticorrosive coating for carbon steel in 3.5% NaCl medium: Combining experimental and computational approaches. *Chem. Phys. Lett.* **2021**, *783*, No. 139081.
(43) El-Aouni, N.; Hsissou, R.; Safi, Z.; Abbout, S.; Benhiba, F.; El Azzaoui, J.; Haldhar, R.; Wazzan, N.; Guo, L.; Erramli, H.; Elharfi, A.; El Bachiri, A.; Rafik, M. Performance of two new epoxy resins as potential corrosion inhibitors for carbon steel in 1MHCl medium: Combining experimental and computational approaches. *Colloids Surf. A: Physicochem. Eng. Asp.* **2021**, *626*, No. 127066.
(44) Hsissou, R.; Azogagh, M.; Benhiba, F.; Echihi, S.; Galai, M.; Shaim, A.; Bahaj, H.; Briche, S.; Kaya, S.; Serdaroğlu, G.; Zarrouk, A.; Ebn Touhami, M.; Rafik, M. Insight of development of two cured epoxy polymer composite coatings as highly protective efficiency for carbon steel in sodium chloride solution: DFT, RDF, FFV and MD approaches. *J. Mol. Liq.* **2022**, *360*, No. 119406.
(45) Dennington, R.; Keith, T. A.; Millam, J. M. *GaussView 6.0. 16*; Semichem Inc.: Shawnee Mission, KS, 2016.
(46) Frisch, M. J.; Trucks, G. W.; Schlegel, H. B.; Scuseria, G. E.; Robb, M. A.; Cheeseman, J. R.; Scalmani, G.; Barone, V.; Mennucci, B.; Petersson, G. A.; Nakatsuji, H.; Caricato, M.; Li, X.; Hratchian, H. P.; Izmaylov, A. F.; Bloino, J.; Zheng, G.; Sonnenberg, J. L.; Hada, M.; Ehara, M.; Toyota, K.; Fukuda, R.; Hasegawa, J.; Ishida, M.; Nakajima, T.; Honda, Y.; Kitao, O.; Nakai, H.; Vreven, T.; Montgomery, J. A.; Peralta, J. E.; Ogliaro, F.; Bearpark, M.; Heyd, J. J.; Brothers, E.; Kudin, K. N.; Staroverov, V. N.; Kobayashi, R.; Normand, J.; Raghavachari, K.; Rendell, A.; Burant, J. C.; Iyengar, S. S.; Tomasi, J.; Cossi, M.; Rega, N.; Millam, J. M.; Klene, M.; Knox, J. E.; Cross, J. B.; Bakken, V.; Adamo, C.; Jaramillo, J.; Gomperts, R.; Stratmann, R. E.; Yazyev, O.; Austin, A. J.; Cammi, R.; Pomelli, C.; Ochterski, J. W.; Martin, R. L.; Morokuma, K.; Zakrzewski, V. G.; Voth, G. A.; Salvador, P.; Dannenberg, J. J.; Dapprich, S.; Daniels, A. D.; Farkas, O., Foresman, J. B.; Ortiz, J. V.; Cioslowski, J.; Fox, D. J. *Gaussian 09, revision D.01*. Gaussian Inc: Wallingford CT, 2009.
(47) Günsel, A.; Bilgiçli, A. T.; Tüzün, B.; Pişkin, H.; Atmaca, G. Y.; Erdoğmuş, A.; Yarasir, M. N. Synthesis of tetra-substituted phthalocyanines bearing 2-(ethyl (m-tolyl) amino) ethanol: Computational and photophysicochemical studies. *J. Photochem. Photobiol., A* **2019**, *373*, 77−86.
(48) Güzel, E.; Günsel, A.; Tüzün, B.; Atmaca, G. Y.; Bilgiçli, A. T.; Erdoğmuş, A.; Yarasir, M. N. Synthesis of tetra-substituted metallophthalocyanines: Spectral, structural, computational studies and investigation of their photophysical and photochemical properties. *Polyhedron* **2019**, *158*, 316−324.
(49) Tüzün, B. Theoretical evaluation of six indazole derivatives as corrosion inhibitors based on DFT. *Turk. Comput. Theor. Chem.* **2018**, *2*, 12−22.
(50) Schrödinger, L. L. C. *Schrödinger Release 2022−3: LigPrep*. Schrödinger Inc.: New York, NY, USA, 2021.
(51) Schrödinger, L. L. C. *Schrödinger release 2019−4: protein preparation wizard; Epik; impact; prime; glide; LigPrep; induced fit docking protocol*. New York, NY, 2019.
(52) Schrödinger, L. L. C. *Schrödinger Release 2021−3: LigPrep*, New York, NY, 2021.
(53) Genç Bilgiçli, H.; Taslimi, P.; Akyuz, B.; Tuzun, B.; Gulcin, I. Synthesis, characterization, biological evaluation, and molecular docking studies of some piperonyl-based 4-thiazolidinone derivatives. *Arch. Pharm.* **2020**, *353*, 1900304.
(54) Schrödinger, L. L. C. *Schrödinger Release 2021−3: QikProp*, New York, NY, 2021.
(55) Krishna, P. M.; Ramachary, D. B.; Peesapati, S. Azide-acetonitrile "click" reaction triggered by Cs2 CO3: The atom-economic, high-yielding synthesis of 5-amino-1, 2, 3-triazoles. *RSC Adv.* **2015**, *5*, 62062−62066.
(56) Günsel, A.; Kırbaç, E.; Tüzün, B.; Erdoğmuş, A.; Bilgiçli, A. T.; Yarasir, M. N. Selective chemosensor phthalocyanines for Pd^{2+} ions, synthesis, characterization, quantum chemical calculation, photochemical and photophysical properties. *J. Mol. Struct.* **2019**, *1180*, 127−138.
(57) Poustforoosh, A.; Hashemipour, H.; Tüzün, B.; Pardakhty, A.; Mehrabani, M.; Nematollahi, M. H. Evaluation of potential anti-RNA-dependent RNA polymerase (RdRP) drugs against the newly emerged model of COVID-19 RdRP using computational methods. *Biophys. Chem.* **2012**, *272*, No. 106564.
(58) Genç Bilgiçli, H.; Taslimi, P.; Akyuz, B.; Tuzun, B.; Gulcin, I. Synthesis, characterization, biological evaluation, and molecular docking studies of some piperonyl-based 4-thiazolidinone derivatives. *Arch. Pharm.* **2020**, *353*, 1900304.
(59) Bytyqi-Damoni, A.; Kestane, A.; Taslimi, P.; Tuzun, B.; Zengin, M.; Bilgicli, H. G.; Gulcin, I. Novel carvacrol based new oxypropanolamine derivatives: Design, synthesis, characterization, biological evaluation, and molecular docking studies. *J. Mol. Struct.* **2020**, *1202*, No. 127297.
(60) Lipinski, C. A. Lead-and drug-like compounds: the rule-of-five revolution. *Drug Discovery Today: Technol.* **2004**, *1*, 337−341.
(61) Lipinski, C. A.; Lombardo, F.; Dominy, B. W.; Feeney, P. J. Experimental and computational approaches to estimate solubility and permeability in drug discovery and development settings. *Adv. Drug Delivery Rev.* **1997**, *23*, 3−25.
(62) Jorgensen, W. J.; Duffy, E. M. Prediction of drug solubility from structure. *Advanced drug delivery reviews* **2002**, *54*, 355−366.
(63) Kategaonkar, A. H.; Shinde, P. V.; Kategaonkar, A. H.; Pasale, S. K.; Shingate, B. B.; Shingare, M. S. Synthesis and biological evaluation of new 2-chloro-3-((4-phenyl-1H-1,2,3-triazol-1-yl)methyl)quinoline derivatives via click chemistry approach. *Eur. J. Med. Chem.* **2010**, *45*, 3142−3146.
(64) Mareddy, J.; Sri Shanthi Praveena, K.; Suresh, N.; Jayashree, A.; Roy, S.; Rambabu, D.; Yadagiri Sreenivasa Murthy, N.; Pal, S. A remarkably faster approach towards 1,2,3-triazolyl quinolines via CuAAC in water: their crystal structure analysis and antibacterial activities. *Lett. Drug Des. Discovery* **2013**, *10*, 343−352.

https://doi.org/10.1021/acsomega.4c03906
ACS Omega 2024, 9, 25395−25409

(65) Thomas, K. D.; Adhikari, A. V.; Shetty, N. S. Design, synthesis and antimicrobial activities of some new quinoline derivatives carrying 1,2,3-triazole moiety. *Eur. J. Med. Chem.* **2010**, *45*, 3803−3810.
(66) Sumangala, V.; Poojary, B.; Chidananda, N.; Fernandes, J.; Kumari, N. S. Synthesis and antimicrobial activity of 1,2,3-triazoles containing quinoline moiety. *Arch Pharm. Res.* **2010**, *33*, 1911−1918.
(67) Singh, H.; Nand, B.; Sindhu, J.; Khurana, J. M.; Sharma, C.; Aneja, K. R. Efficient one pot synthesis of xanthene-triazole-quinoline/phenyl conjugates and evaluation of their antimicrobial activity. *J. Braz. Chem. Soc.* **2014**, *25*, 1178−1193.
(68) El-Bindary, M. A.; El-Bindary, A. A. Synthesis, characterization, DNA binding, and biological action of dimedone arylhydrazone chelates. *Appl. Organomet. Chem.* **2022**, *36*, No. e6576.
(69) El-Zahed, M. M.; Diab, M. A.; El-Sonbati, A. Z.; Saad, M. H.; Eldesoky, A. M.; El-Bindary, M. A. Synthesis, spectroscopic characterization studies of chelating complexes and their applications as antimicrobial agents, DNA binding, molecular docking, and electrochemical studies. *Appl. Organomet. Chem.* **2024**, *38*, No. e7290.

https://doi.org/10.1021/acsomega.4c03906
ACS Omega 2024, 9, 25395−25409